

## High field MR Microimaging Investigation Gives More Insights on Spongy Bone Characteristics

*Silvia De Santis,<sup>1,2</sup> Giulia Di Pietro,<sup>1</sup> Mauro Rebuffi,<sup>1,2</sup> Silvia Capuani<sup>1,2</sup>*

<sup>1</sup> Physics Department *Sapienza* University of Rome, Rome Italy

<sup>2</sup> CNR IPCF UOS Roma, Rome, Italy.

Corresponding author: Silvia Capuani, Physics Dept. Sapienza University of Rome, Piazzale Aldo Moro 5, 00185, Rome, Italy. E-Mail: [silvia.capuani@roma1.infn.it](mailto:silvia.capuani@roma1.infn.it)

(received 13 September 2010, accepted 10 January 2011)

### Abstract

Spongy-bone is a porous system characterized by a solid trabecular network immersed in bone-marrow and characterized by a different relative percentage of water and fats. In our previous paper, we demonstrated using calf bone samples, that water is more prevalent in the boundary zone while fats are rearranged primarily in the central zone of each pore. Moreover we showed that water internal gradient ( $G_i$ ) magnitude from the samples was directly proportional to their trabecular bone density. Using a 9.4T MR micro-imaging system, here we evaluated  $T_2$ ,  $T_2^*$ , apparent diffusion coefficient ( $ADC$ ) and  $G_i$  parameters from *in vitro* calf samples in spatially resolved modality, for both water and fat components. Moreover, relative percentages of water and fats were quantified from spectra.  $T_2$ ,  $T_2^*$  and  $ADC$  values are higher in fat than in water component. Moreover, the differential effects of fat and water diffusion result in different  $T_2$  and  $G_i$  behaviours. Our results suggest that differently from fat parameters, water  $T_2^*$ ,  $ADC$  and  $G_i$ , may be reliable markers to assess not only trabecular bone density but, more generally, the status of spongy bone.

### Keywords

Trabecular bone, bone marrow, micro-MRI, internal gradient, diffusion

### 1. Introduction

Spongy-bone is a porous system characterized by a solid trabecular network immersed in bone-marrow and characterized by different relative percentages of water and fats. The main attention in spongy bone investigations is related to the interest in identifying parameters and procedures with the ability to assess the spongy bone status, thus contributing to osteoporosis diagnosis. Indeed, bone mineral density (BMD) measurement, which is currently considered the gold standard for clinical diagnosis of osteoporosis [1], is an inadequate sole predictor of bone fracture risk [2,3], suggesting that other factors besides the low BMD likely contribute to determine bone fragility. This lack of information on the risk of bone fracture, has prompted intense research to identify new parameters with the ability to detect spongy bone status and to provide reliable measures of bone

resistance. Several Magnetic Resonance (MR) techniques have thus been developed to assess spongy bone status, such as MR interferometry [4,5,6] and the  $\mu$ -MRI [7,8]. The former is based on  $T_2^*$ -weighted Gradient Echo imaging and  $T_2^*$  quantification of the spongy bone marrow. The latter relies instead on high resolution MR Imaging, which allows a quantitative morphometric analysis of the three-dimensional structure of trabecular bone (TB). Some years ago we presented the first high-field diffusion images of bone marrow in spongy bone samples [9,10] while, very recently, we proposed a new Magnetic Resonance (MR) strategy based on the evaluation of internal gradient ( $G_i$ ) as extracted from the Spin-Echo decay function to assess the TB density in spongy bone [11]. These papers underlined that the mean  $ADC$  in spongy bone samples from bovine was of the order of  $10^{-10} \text{m}^2/\text{s}$  [9,10] and emphasized that differences between smaller and larger pores in spongy bone are better characterized by means of diffusion weighted images as compared to  $T_2$ -weighted images. Moreover, in these diffusion experiments the selected diffusion length was approximately less than  $10 \mu\text{m}$ , namely less wide than the average dimension of pores in bovine spongy bone (equal to  $50\text{-}300 \mu\text{m}$ ). Finally, we demonstrated [11] in calf bone samples, that water is more prevalent in the boundary zone while fats are rearranged primarily in the central zone of each pore. Furthermore we showed that water internal gradient ( $G_i$ ) magnitude from the samples was directly proportional to their TB density [11].

On the base of these observations  $T_2$ ,  $T_2^*$ ,  $ADC$  and  $G_i$  measurements for both water and fat components in calf bone samples are illustrated and discussed here to characterize spongy bone.

## 2. Methods and Materials

We investigated, at 9.4T magnetic field, spongy bone specimens from femoral head of calves, using a micro-imaging probe equipped with maximum gradient strength of  $1200 \text{mT/m}$ .  $T_2$ ,  $T_2^*$ ,  $ADC$  and  $G_i$  were measured in spatially resolved modality (in plain image resolution equal to  $40 \mu\text{m}$ , slice thickness  $250 \mu\text{m}$ ) for both water and fat components. Mean values (and their standard deviation,  $SD$ ) of the aforementioned parameters were obtained performing an average over values extracted from 4 slices. Six ex-vivo spongy bone specimens ( $20\text{mm}$  high,  $6\text{mm}$  deep) excised from femoral head of calves (4 specimens) and from distal femur (2 specimens), were cut into three pieces of approximately  $7\text{-}6\text{mm}$  high and  $5\text{mm}$  deep, in order to obtain, for each specimen, three samples characterized by different TB densities (see figure 1). Sample temperature was fixed to  $291 \text{K}$ . Gradient Echo images were obtained to evaluate  $T_2^*$ , using GEFI imaging sequence ( $TR=1000\text{ms}$ ,  $NS=16$ ) at various  $TE$ s (from  $1.8$  to  $60\text{ms}$ ). A MSME (Multi Slice Multi Echo) imaging sequence ( $TR=2000\text{ms}$ ,  $NS=8$ ) at various  $TE$ s (from  $2.8$  to  $120\text{ms}$ ), was used to obtain SE decay. Both  $T_2$  and  $G_i$  were evaluated from the attenuation of SE signal as a function of different  $TE$ s. A Pulse Gradient STimulated Echo (PGSTE) imaging sequence was also employed ( $TE/TR=21.9/3000\text{ms}$ ,  $\Delta=80\text{ms}$ ,  $\delta=4\text{ms}$ , using eight b-values ranging from  $200$  to  $80000\text{s/mm}^2$ ,  $NS=16$ ) in order to measure  $ADC$  along x axis. Spectra were also obtained to evaluate water and fat percentage from each sample. To obtain  $T_2$ ,  $T_2^*$ ,  $ADC$  and  $G_i$  for both fat and water, a Levenberg-Marquard fit was performed using the signal as a superimposition of the two bone marrow components.

The behaviour of all aforementioned MR parameters was investigated as a function of: 1) samples TB density, 2) relative water concentration in bone marrow. To quantify TB density, we calculated the ratio between the perimeter and the area of each pore in the slices. As a result, the ratio ( $N_p/N_a$ ) between number of voxels defining each pore perimeter ( $N_p$ ) and number of voxels constituting the corresponding area ( $N_a$ ) was obtained from all pores included in each of the slices. As a consequence, bone samples characterized by  $N_p/N_a$  values ranging from:  $0.35$  to  $0.55$ ,  $0.31$  to  $0.34$ ,  $0.28$  to  $0.30$  and  $0.24$  to  $0.27$  were indicated as HTD (higher TB), ITDa (intermediate TB), ITDb (intermediate TB) and LTD (lower TB), respectively (see Fig. 1).

### 3. Results

Figure 2 displays the different behaviour of water and fat measured MR parameters as a function of both TB density and water percentage in bone marrow ( $W\%$ ). Water  $T_2$ ,  $T_2^*$  and  $ADC$  are characterized by a decreasing trend when moving from lower TD to higher TB and water  $G_i$  increases proportionally with the increase in TB density. Conversely, fat  $G_i$ , fat  $ADC$  and fat  $T_2^*$  as a function of TB density, do not show a specific trend. Fat  $ADC$  values result to be independent on both TB density and  $W\%$ , while fat  $T_2$  decreases proportionally with the increase in both TB density and  $W\%$ . Water  $T_2$ ,  $T_2^*$ ,  $ADC$  and  $G_i$  values extracted from femoral head of calves showed in Fig.2, must be compared with water  $T_2$ ,  $T_2^*$ ,  $ADC$  and  $G_i$  values extracted from a distal femur samples listed in Table 1.

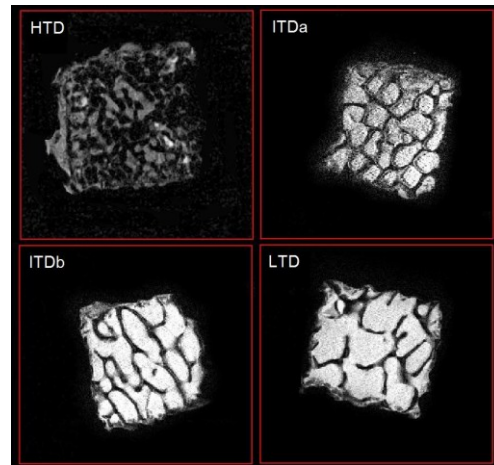


**Fig. 1:** An example of calf spongy bone specimens used. SE image slices ( $TE=4ms$ ) obtained from: closely spaced spongy bone samples (HTD), intermediate trabecular bone density samples (ITDa, ITDb) and larger inter-trabecular samples (LTD).

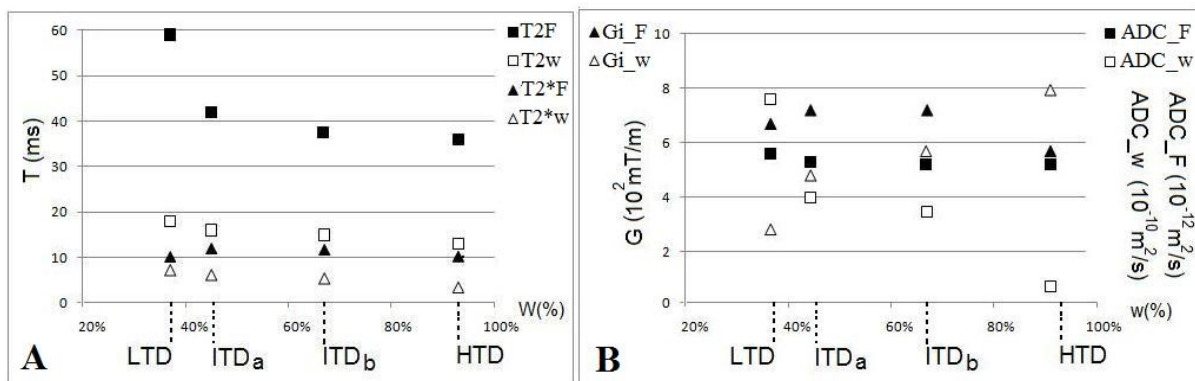


**Fig. 2** Results from femoral head samples. A) Fat  $T_2$  and  $T_2^*$  (filled squares and triangles, respectively) and water  $T_2$  and  $T_2^*$  (empty squares and triangles, respectively) as a function of both TB density (LTD, ITDa, ITDb, HTD) and water percentage in bone marrow ( $W\%$ ). B) Fat  $G_i$  and  $ADC$  (filled squares and triangles, respectively) and water  $G_i$  and  $ADC$  (empty squares and triangles, respectively) as a function of both TB density (LTD, ITDa, ITDb, HTD) and  $W\%$ .

Again, water  $T_2^*$  is characterized by a decreasing trend when moving from LTD to HTB, however  $T_2^*$  values in table 1 are lower than those displayed in Fig.2. Furthermore water  $G_i$

	%Water	$(T_2^* \pm SD)ms$	$(T_2 \pm SD)ms$	$(ADC \pm SD) * 10^{-10} m^2/s$	$(G_i \pm SD)mT/m$
LTD	15	$6.9 \pm 1.0$	$15.0 \pm 1.0$	$0.9 \pm 0.2$	$522 \pm 331$
ITDb	28	$5.2 \pm 0.5$	$16.2 \pm 1.0$	$1.7 \pm 0.3$	$782 \pm 134$
HTD	57	$4.0 \pm 0.5$	$15.9 \pm 1.0$	$3.2 \pm 0.1$	$1093 \pm 281$

**Table 1.** Results from one distal femur specimen: water component.

displayed in Table 1 increase proportionally with the increase in TB density, showing higher values as compared to  $G_i$  values displayed in Fig.2. Conversely water  $ADC$  values displayed in Table 1 compared to those in Fig.2 showed an opposite behaviour as a function of TB density.  $ADC$  behaviour depends on either  $W\%$  (or fat content) or TB density.

## 4. Discussion

Data illustrated here demonstrate the key role of diffusion to obtain both structural and quality information from spongy bone. Fat  $ADC$  is approximately two orders of magnitude less than water  $ADC$ , and the former results to be independent on both TB density and  $W\%$ . Conversely, water  $ADC$  is characterized by a fast (of the order of  $10^{-9} \text{ m}^2/\text{s}$ ) or a restricted (of the order of  $10^{-10}$  -  $10^{-11} \text{ m}^2/\text{s}$ ) diffusion regime as a function of fat quantity. Considering that water is more prevalent in the boundary zone, while fats are rearranged primarily in the central zone of each spongy bone pore [11] it is possible to understand the important role of water diffusion to characterize spongy bone. Water diffusion partially averages the rapid spin dephasing effect due to susceptibility difference between bone and water. The faster the diffusion, the higher the average effect. As a consequence water  $T_2^*$  and water  $G_i$  values related to a selected TB density, strongly depend on water diffusion regime. Besides, in spongy bone, water diffusion regime is strictly linked to the width of the boundary pore zone (between solid bone and fat), where water is more prevalent. The smaller the boundary zone, the lower the average effect. Data reported in Table 1 and Fig.2 can be fully explained using the above argumentations. As an example, because distal femur specimens are characterized by a higher fat content compared to that of femoral head samples, water diffusion regime is more restricted in samples of Table 1 than in those displayed in Fig.2. As a consequence, for a fixed TB density,  $T_2^*$  in Table 1 is lower than  $T_2^*$  in Fig.2. Moreover,  $G_i$  in Table 1 is higher than  $G_i$  in Fig.2.

## 3. Conclusions

$T_2^*$ ,  $ADC$  and  $G_i$  extracted from bone marrow water component and, more strongly, water  $G_i$  may be reliable markers to evaluate trabecular bone density and to assess the status of spongy bone. Conversely  $T_2^*$ ,  $ADC$  and  $G_i$  from fat component did not provide any useful information related to TB density.

## References

- [1] J.A. Kanis and C.C. Gluer, *Osteop. Interl.* 11 (2000) 192-202.
- [2] J.A. Kanis, *Lancet* 359 (2002) 1929-36.
- [3] F.W. Wehrli, L. Hilaire, M. Fernández-Seara, B.R. Gomberg, H. Kwon Song, B. Zemel, L. Loh and P.J. Snyder, *J. Bone Min. Res.* 17 (2002) 2265-73.
- [4] F.W. Wehrli, J.C. Ford, M. Attie, H.Y. Kressel, F.S. Kaplan, *Radiology* (1991) 179 615-621
- [5] F.W. Wehrli, J.A. Hopkins, S.N. Hwang, H.K. Song, P.J. Snyder, J.G. Haddad, *Radiology* 217 (2000) 527-538.
- [6] T.M. Link, S. Majumdar, P. Augat, et al. *Radiology* 209 (1998) 531-536.
- [7] P.K. Saha, B.R. Gomberg, F.W. Wehrli. *Int. J. Imag. Syst. Tech.* 11 (2000) 81-90.
- [8] R. Krug, S. Banerjee, E.T. Han, D.C. Newitt, T.M. Link, S. Majumdar, *Osteop. Int.* 16 (2005) 1307-1314.
- [9] S. Capuani, C. Rossi, M. Alesiani, B. Maraviglia, *Solid State NMR*, 28 (2005) 266-272.
- [10] C. Rossi, S. Capuani, F. Fasano, M. Alesiani, B. Maraviglia, *Magn. Reson. Imag.* 23 (2005) 245-248.
- [11] S. De Santis, M. Rebuzzi, G. Di Pietro, F. Fasano, B. Maraviglia, S. Capuani, *Phys. Med. Biol.* 55 (2010) 5767-5785.